

1 **Methods**

2

3 **CASS Barcode generation**

4 The initial 20-base pair (bp) barcode candidates were generated through random combinations of
5 the four nucleotides (A, T, C, G) in silico. All candidate sequences were then filtered using the
6 online BLAST tool by comparing them against the RefSeq database. Sequences with a similarity
7 score within the lowest 0.1% of all hits were selected. Subsequently, a second round of BLAST was
8 performed on the chosen candidates to ensure that no pair of sequences shared more than seven
9 identical base pairs, and to confirm the absence of significant similarity between any sequences.

10 This in silico selection process resulted in 46 candidate sequences. To further refine these, an in
11 vitro selection was conducted. As outlined in panel 2 of Extended Data Fig. 1A, plasmids expressing
12 the selected candidates were transfected into 293T cells, and corresponding probes were used for
13 hybridization. Data from these experiments are also presented in Extended Data Fig. 2. Candidates
14 exhibiting non-specific binding or weak fluorescence signals were discarded.

15 To assess the non-specificity of the probes with respect to endogenous RNA, additional
16 hybridization experiments were performed on wild-type mouse brain sections. Only probes that
17 failed to produce any signal were selected.

18 Following both the in silico and in vitro selection processes, 24 short sequences were identified and
19 selected as the final elements of the CASS barcode.

20

21 **Construction of barcoded viral plasmids**

22 To generate the barcode plasmids, we employed commercial chemical gene synthesis. However,
23 synthesizing the entire pool using this method would be prohibitively expensive. Therefore, we
24 divided the CASS barcode into two parts: Part 1 (containing sequences ABCD) and Part 2
25 (containing sequences EFGH). Each part consisted of $3^4 = 81$ possible combinations, and 81
26 fragments from each part (162 total) were synthesized using commercial gene synthesis services
27 (Sangon and Dynegene).

28 The plasmid for Part 1 was constructed by inserting it into the SAD-RV-dG-BFP vector (generated
29 in our laboratory). Part 2 was amplified by PCR (Takara, R045A) and subsequently digested with
30 restriction enzymes (NheI and SbfI, NEB, R3131 and R3642). The digested PCR product from Part

31 2 was then ligated into the plasmid vector of Part 1 via traditional restriction digestion and ligation
32 (NEB, M0202).

33 Both parts were divided into nine equimolar groups, and 81 ligation reactions were performed, each
34 containing one of the 81 potential products. The ligation products were introduced into competent
35 E. coli cells (Accurate Biology, AG11804) through transformation. The transformed E. coli cells
36 were cultured on 15 cm diameter plates (JET BIOFIL, TCD010150) containing low-salt LB medium
37 (0.5% NaCl, 1% yeast extract, 1% tryptone, 2% agar) and 0.01% ampicillin (BBI Life Sciences ,
38 A610028-0025). Plasmids were then extracted from bacterial cultures using the plasmid extraction
39 kit (Macherey-Nagel, 740426.5).

40

41 **One-step rabies virus packaging and tittering**

42 BHK-EnVA cells were cultured in DMEM (Yeasen, 41401ES76) supplemented with 10% FBS
43 (Yeasen, 40131ES76) at 37°C in a 5% CO₂ atmosphere. Cells were grown to 80% confluence prior
44 to transfection.

45 The plasmid library of RV-BFP-CASS barcode was divided into nine groups, each containing 273
46 theoretical variants. Each transfection reaction included 45.6 μ g RV backbone, 5.8 μ g CAG-T7
47 polymerase, 9 μ g CAG-N, 4.7 μ g CAG-P, 4 μ g CAG-L, 2.5 μ g CAG-TVA, 4.8 μ g CAG-EnVA. The
48 plasmid mixes were purified using isopropanol precipitation with an ethanol wash and then
49 dissolved in electroporation buffer (120mM KCl, 0.15mM CaCl₂, 1.3Mm KH₂PO₄, 8.7mM K₂HPO₄,
50 25mM HEPES, 2mM EGTA, 5mM MgCl₂, 2mM Na₂ATP, 5mM Glutathione, filtered through a
51 0.23 μ m filter).

52 For electroporation, BHK-EnVA cells were trypsinized and resuspended in DMEM with 10% FBS.
53 Cells were pelleted by centrifugation, then resuspended in ice-cold electroporation buffer. The
54 plasmid mixture was added to the cell suspension, followed by additional electroporation buffer to
55 reach a final volume of 100 μ L. This mixture was transferred to an ice-cold electroporation cup
56 (Bio-Rad, 1652088-1). Electroporation was performed using an electroporator (BEX, CUY21EDIT
57 II) with the following settings: 250 V for 10 ms (ON) and 5 ms (OFF), followed by a 40 V square
58 wave pulse for 50 ms repeated 10 times. Before electroporation, the resistance was verified to be
59 approximately 200 Ω . After electroporation, the cells were placed on ice, and fresh DMEM with
60 10% FBS at 37°C was added to resuspend the cells. The cells were then transferred to a 75 cm²

61 culture flask (JET BIOFIL, TCF012250) and cultured at 37°C in 5% CO₂ for 48 hours. The day of
62 electroporation was designated as Day 0.

63 On Day 2, the culture medium was replaced. On Day 4, the medium was replaced again, and the
64 cells were moved to a 34°C, 3% CO₂ incubator. By Day 5, BFP⁺ cells were observable, and the
65 medium was collected and stored at 4°C, with fresh DMEM added. Cells were trypsinized and
66 transferred to a 15 cm diameter culture plate (JET BIOFIL, TCD010150) pretreated with poly-D-
67 lysine (Beyotime, ST508). Medium was collected daily from Day 6 to Day 8 and stored at 4°C with
68 fresh medium added to the cells each day.

69 On Day 8, the collected medium from Days 5 to 8 for each transfection group was pooled, treated
70 with 30 U/mL Benzonase (Servivebio, G3406-50KU), and incubated at 37°C for 20 minutes. The
71 supernatant was filtered through a 0.45 µm filter (JET BIOFIL, FPV403250) to remove debris.

72 For ultracentrifugation, the filtered supernatant was added to an ultracentrifuge tube (Beckman
73 Coulter, 344058), followed by 5 mL of 20% sucrose, and the mixture was centrifuged at 4°C at
74 20,000 rpm for 2 hours (Beckman Coulter, SW32Ti rotor). After centrifugation, the supernatant was
75 discarded, and the resulting pellet was resuspended in 30 µL of PBS per tube, with gentle shaking
76 at 4°C overnight. The virus solution was then collected for titering, and the remaining solution was
77 stored at 4°C. At this stage, nine separate virus libraries were obtained, each containing 273 variants
78 in theory.

79 For virus titering, serial dilutions (10⁻¹, 10⁻², etc.) of the virus were added to the culture medium of
80 293T-TVA cells in a 24-well plate (JET BIOFIL, TCP011024). After 2 days, the dilution yielding
81 approximately 100 sparse BFP⁺ cells was selected. BFP⁺ cells were counted in 10 randomly selected
82 fields under a 10X objective, and the virus titer was calculated. The nine virus splits were then
83 pooled in equimolar amounts, aliquoted, and stored at -80°C for quality control and subsequent
84 injections.

85

86 **Virus quality control**

87 **Library construction**

88 To extract RNA from virus samples, 4µL of virus, 200µL of TRIzol (Invirogen, 15596018CN), and
89 1µL of glycogen (Thermo Scientific, R0551) were mixed thoroughly by pipetting. After a 5-minute
90 incubation, 40 µL of chloroform (CHCl₃) was added, and the mixture was centrifuged at 14,000 rpm

91 for 15 minutes at 4°C. The aqueous phase was carefully collected, and RNA was precipitated by
92 adding 100µL of isopropanol. The solution was then centrifuged again at 14,000 rpm for 15 minutes
93 at 4°C. Afterward, the RNA pellet was washed twice with 75% ethanol, followed by a final
94 resuspension in 10µL of RNase-free water.

95 Reverse transcription was performed using the Maxima H Reverse Transcriptase Kit (Invitrogen,
96 EP0753) according to the manufacturer's protocol. The reverse transcription primer, which
97 included unique molecular identifiers (UMIs) with an eight-nucleotide random sequence
98 (NNNNNNNN), was as follows:

99 CCTACACGACGCTCTCCGATCTNNNNNNNNGTGGCCATTACGGCCGGCGCGC.

100 The reverse transcription product was then subjected to the first PCR amplification for NGS
101 library construction using the PrimeSTAR Kit (Takara, R045A) with 25 cycles. The annealing
102 temperature was set to 58°C. The forward primer used was CCTACACGACGCTCTCCGATCT,
103 and the reverse primer was

104 TCAGACGTGTGCTCTCCGATCTCGACTGAAAAGCTAGTGCTAAGCGGCCGC. PCR
105 products were purified using the SPRIselect reagent (Yeasen, 12601ES08) according to the
106 manufacturer's instructions (0.7X, collecting DNA fragments >550 bp).

107 The purified products were then subjected to a second PCR amplification using the PrimeSTAR
108 Kit (Takara, R045A) with 10 cycles. The annealing temperature was again 58°C. The forward
109 primer used was

110 AATGATACGGCGACCACCGAGATCTACACACACTCTTCCCTACACGACGC, and the
111 reverse primer was

112 CAAGCAGAAGACGGCATACGAGATTGAATGTAGTGACTGGAGTTCAGACGTGTGCT.

113 After amplification, the products were purified using SPRIselect (0.5X + 0.2X, collecting DNA
114 fragments within the range of 550–900 bp).

115 Finally, the purified NGS library was sent for next-generation sequencing (Mingmatechs, Illumina
116 Nova6000 S4, index i7 = GAAACACA).

117

118 **Data analysis**

119 The raw “.fastq” sequencing data was utilized for virus quality control. All data analysis was
120 performed using custom scripts written in MATLAB R2018b (MathWorks), and the corresponding

121 code is provided in the supplementary files (folder NGS).
122 The data were initially filtered to ensure that the Q30 score was greater than 90. The unique
123 molecular identifiers (UMIs), as specified in the reverse transcription primer, were then extracted.
124 Due to the distinct design of the CASS barcode (Extended Data Fig. 1b), the 5' 150 bp sequence
125 captured the ABCD region, while the 3' 150 bp sequence covered the EFGH region. The barcode
126 information was subsequently extracted, and the frequency of each barcode was calculated based
127 on UMI counts (Fig. 2b, c).

128 For uniqueness estimation (Fig. 2d), barcodes were randomly selected from the pool in multiple
129 iterations (particles). Each barcode was checked for uniqueness within the selected group, and the
130 final result was based on the average of 1000 simulations.

131 For optimization of injection titer and volume (Fig. 2e), we simulated the random selection of
132 barcodes from 1 to 1000, evaluating whether all the selected barcodes were unique. The probability
133 of achieving uniqueness was calculated from 1000 simulation trials.

134

135 **Mice and injection**

136 All animal procedures were conducted in strict accordance with the approved protocols from the
137 Animal Care and Use Committee of the Center for Excellence in Brain Science and Intelligence
138 Technology, Institute of Neuroscience, Chinese Academy of Sciences, and the committee at Lingang
139 Laboratory. The mice were housed in groups under standard laboratory conditions. *Neurod6-cre*
140 mice were maintained as heterozygotes on a C57BL/6 background.

141 As outlined in Extended Data Fig. 1d, three mice were used in the connectome study of the visual
142 cortex. The injection coordinates for each mouse were as follows: mouse #1, AP -1.99 mm, ML -
143 3.22 mm, DV 0.40 mm; mouse #2, AP -1.75 mm, ML -2.95 mm, DV 0.40 mm; and mouse #3, AP -
144 1.91 mm, ML -3.11 mm, DV 0.40 mm. The Bregma point was defined as AP 0 and ML 0, and the
145 pial surface was defined as DV 0.

146

147 **Sample pre-treatment**

148 Three or four brain slices were processed at a time. All solutions used were RNase-free, and
149 procedures were conducted in a clean, RNase-free environment, with most steps carried out under
150 a laminar flow hood. The brain slices were first incubated separately in 4% PFA (Coolaber, SL1830)

151 in 24-well plates for 15 minutes, followed by three washes with PBS. The slices were then incubated
152 in 8% SDS (dissolved in PBS) at room temperature with gentle shaking for 40 minutes, followed
153 by three washes with PBS.

154 Subsequently, the slices were transferred to chambered glass slides (Cellvis, C1-1.5H-N), which had
155 been pre-treated with 0.02 mg/ml Poly-D-lysine (Beyotime, ST508) overnight at room temperature.
156 The slices were gently attached to the chambered glass using a clean brush in PBS. After aspirating
157 the PBS, the chambered glass was quickly dried using a hair dryer. The sample (three or four slices
158 on the chambered glass) was then incubated in 4% PFA with gentle shaking at room temperature for
159 10 minutes, followed by three washes with PBS.

160 Fluorescence signals for BFP, mCherry, and E2Crimson were captured using confocal microscopy
161 (Olympus, FV3000) to identify the starter cells. Following imaging, the sample was incubated in
162 Wash Buffer 1 (30% deionized formamide (BBI, A600211), 2 mM Ribonucleoside-Vanadyl
163 Complexes (RVC, BBI, B644221) in 2X SSC solution) at 50°C for 5 minutes. The wash buffer was
164 aspirated, and the sample was then incubated with Hyb Buffer 1 (30% deionized formamide, 2 mM
165 RVC, 0.2 mg/ml salmon sperm DNA (Sigma, D7656), 1 mg/ml yeast tRNA (Acme, T48660), and
166 10% w/v dextran sulfate (Santa Cruz, sc-203917) in 2X SSC solution). A HybriSlip hybridization
167 cover (Electron Microscope Sciences, 70329) was placed over the sample to prevent evaporation.
168 The sample was incubated at 50°C for 4 hours, then allowed to cool to room temperature and stored
169 overnight.

170 On the following day, the sample was washed in Wash Buffer 1 at 55°C, and the HybriSlip was
171 removed. After aspirating Wash Buffer 1, the sample was incubated with fresh Wash Buffer 1 at 55°C
172 for 30 minutes, followed by three washes with 2X SSC at room temperature. The sample was then
173 incubated in 4% PFA with gentle shaking at room temperature for 10 minutes, followed by three
174 additional washes with 2X SSC. The sample was then placed in 2X SSC for pre-bleaching.
175 The pre-bleaching step was performed using an LED laser (FluoCa, FC904) with a 420 nm long-
176 pass optical filter on a BX51 microscope. Using a 10X air objective, a region of interest was
177 bleached for 15 minutes. Once all regions of interest had been bleached, the sample was ready for
178 barcode FISH.

179

180 **Barcode fluorescence in situ hybridization**

181 The probes were chemically synthesized with a 5' fluorescent dye (Alexa488 for 488, Cy3 for 561,
182 and Cy5 for 647) by a commercial primer synthesis service (Sangon). The probes were dissolved in
183 RNase-free water to a 100 μ M stock concentration and stored at -80°C. For temporary use, the probes
184 were diluted to 10 μ M and stored at 4°C. A mixture of three probes was prepared in Hyb Buffer 2
185 (5% deionized formamide, 2 mM RVC, and 10% w/v dextran sulfate in 2X SSC) at a final
186 concentration of 10 nM for each probe.

187 For each cycle, the liquid was first aspirated, followed by the incubation of probes (approximately
188 500 μ L per chambered glass) at 37°C for 20 minutes. After incubation, the probes were aspirated,
189 and the sample was washed three times with Wash Buffer 2 (5% deionized formamide in 0.2X SSC)
190 at 37°C, with each wash step lasting 2 minutes. Finally, approximately 2 mL of Wash Buffer 2 was
191 left to infiltrate the sample. Following washing, fluorescent probes hybridized to their corresponding
192 RNA targets, and a Z-stack image was captured using an inverted confocal microscope (Olympus,
193 FV3000) with a 20X air objective (NA 0.8). An additional bright-field image of the entire sample
194 was captured during the first cycle to facilitate subsequent alignment with the Allen Brain Atlas.

195 The Z-axis was set to the middle of the sample, and a photobleaching step was performed using the
196 “stimulation” module in FV3000 software with the same objective. In this step, the selected lasers
197 (488, 561, and 647 nm) were turned on, while the GaAsP PMT detector was turned off. Typically,
198 the entire imaging area was selected as the bleaching region; however, if the signal was only present
199 in a part of the view, the bleaching region was defined as a region of interest (ROI). Photobleaching
200 was carried out for 15 minutes per view (optical power is around 3.0mW/mm² for each channel at
201 the objective lens), which was sufficient to quench the fluorescence of the probes. After
202 photobleaching, the next cycle was initiated.

203 For manual 8-cycle FISH, the sample may be removed from the microscope, so a manual check of
204 the view is necessary between cycles. For automated FISH, the sample remains in place until the
205 completion of all 8 cycles, with only micron-level shifts occurring. These shifts can be corrected
206 during the subsequent data analysis process.

207 Decoding accuracy is defined as the fraction of cells that are fully decoded in each cycle. The
208 accuracy in each cycle remains constant (Extended Data Fig. 4d), suggesting that there was no
209 interference of preexisting probes on newly added ones.

210

211 **Immunofluorescence labelling**

212 Immunofluorescence labeling was applied to samples after the completion of the 8-cycle FISH
213 procedure. Initially, the samples were washed three times with PBS, with each wash lasting 10
214 minutes. The samples were then incubated in blocking buffer (5% BSA (Sigma, V900933), 0.5%
215 Triton X-100 (Aladdin, T109027) in PBS) for 2 hours at room temperature with gentle shaking.
216 Following blocking, the samples were incubated overnight at 4°C with rabbit anti-somatostatin
217 antibody (Invitrogen, PA585759) at a 1:1500 dilution in blocking buffer, with gentle shaking.
218 On the following day, the samples were rinsed three times with PBS, with each rinse lasting 10
219 minutes. Subsequently, the samples were incubated with donkey anti-rabbit secondary antibody
220 conjugated to a 647 nm fluorescence dye (A-31573) for 4 hours at room temperature, with gentle
221 shaking. Afterward, the samples were washed three times with PBS, each wash lasting 10 minutes,
222 prior to imaging.

223 The images were collected using an inverted confocal microscope (Olympus, FV3000). The same
224 imaging region for FISH was manually selected based on BFP signals. Somatostatin-positive cells
225 were identified manually in the resulting images.

226

227 **Barcode decoding**

228 **Coordinate Alignment with Allen Brain Atlas**

229 Each brain slice was aligned to the Allen Brain Atlas (Allen CCF v3)¹ using the QuickNII² software
230 (NITRC). The bright-field image, captured during the first cycle of each sample, was manually
231 aligned to the standard mouse brain template. QuickNII provides a linear coordinate system,
232 allowing for the calculation of a transformation matrix that enables the mapping of all pixels to the
233 standard brain coordinate system for each slice.

234 The primary source of potential alignment error occurs during this step. We estimated that the
235 maximum positional error for each cell was approximately 100µm, particularly along the anterior-
236 posterior axis, due to the limitations of the coordinate transformation method.

237 **Cellpose3-based cell segmentation**

238 Cycle 5 was selected as the template, with the 405 nm channel (BFP) of the cycle 5 image chosen
239 for cell mask generation. A 3D cell mask was generated using Cellpose3³ with a pre-trained model,
240 achieving approximately 80% accuracy. Manual verification was performed to refine and output the

241 cell masks for each image.

242 **Shift correction**

243 Micron-level XYZ shifts in the sample during the 8-cycle FISH were corrected. As described earlier,
244 cycle 5 was used as the template. The MATLAB function “imregtform” was employed to estimate
245 and correct these shifts. Following this correction, the cell mask generated from cycle 5 was applied
246 consistently across all cycles for decoding.

247 **Decoding score and reliability**

248 Initially, a small region devoid of fluorescence was designated as the background ROI. Pixel values
249 for all 3D cell ROIs (including the background ROI) were calculated for each channel and cycle.
250 The decoding score was defined as the ratio of the mean intensity of the cell ROI to the standard
251 error of the background ROI. Statistical significance was determined using a Student’s t-test with
252 FDR correction (Benjamini-Hochberg method). A cycle was flagged as a “missing cycle” for a cell
253 ROI if no channel in that cycle exhibited significant differences from the background (Extended
254 Data Fig. 4c, d). Only ROIs with significant differences were used for outputting decoding results
255 and reliability assessments.

256 For decoding, a single channel (e.g., a1) was identified as the decoding result if its mean intensity
257 exceeded the sum of the other two channels (e.g., a2 and a3) and showed a significant difference
258 from the background. If no channel exhibited a dominant intensity, the cell was classified as
259 containing “multiple barcodes.”

260 To guide manual verification, a reliability value of 0 or 1 was assigned to each cell ROI in each
261 cycle. 1 indicated no need for manual checking and required strict criteria: decoding score for
262 channel a1 must satisfy the following conditions:

263 1. $a1 > 2 \times (a2 + a3)$

264 2. $a1 > 2$

265 3. $a2 < 1$

266 4. $a3 < 1$

267 Approximately 60% of ROI*cycles passed this stringent criterion, with the remainder subjected to
268 manual review. Cycles with a reliability score of 1 were also verified, and no mis-decoding errors
269 were identified.

270 **Location of cell**

271 The XYZ coordinates (image location) of each cell were determined using the 3D ROI “centroid”
272 property via the MATLAB function “regionprops3”. The corresponding image region (a square)
273 within the entire coronal section was manually identified. Each cell’s location was then mapped to
274 the coronal section (coronal section location) based on the image region. Subsequently, the coronal
275 section location was transformed into the Allen Brain Atlas coordinate system using the
276 transformation matrix described previously. A 3D model was generated using the BrainMesh⁴ app
277 in MATLAB.

278

279 **Connectivity detection**

280 After decoding, the location and barcode information for each cell were obtained. Starter cells were
281 manually identified based on marker expression: cells expressing RV, TVA, and RVG were classified
282 as starters; cells expressing RV and TVA were classified as “TVA only”; and cells expressing RV
283 and RVG were classified as “G only”. These starter cells were then linked to their respective barcode
284 and location information. Unique barcode identification was performed within each experimental
285 set. All RVG-expressing cells (including both starter and “G only” cells) were considered for unique
286 barcode identification. Barcodes expressed in only one RVG-expressing cell were classified as
287 “unique”. Starter cells were subsequently divided into three groups: those with multiple barcodes,
288 unique barcodes, and non-unique barcodes (Extended Data Fig. 4b).

289 Next, input cells were analyzed for the expression of unique barcodes. This included input cells with
290 one or two missing cycles, which were accounted for using wildcard matching (fault-tolerant
291 algorithms). For instance, if an input cell expressed the barcode 01111112 (with 0 indicating a
292 missing cycle) and a starter cell expressed 31111112 while no RVG-expressing cells expressed
293 11111112 or 21111112, the input cell was matched to the starter cell, and the corresponding barcode
294 was identified as unique or non-unique. Fully decoded cells were further matched against the pool
295 of unique starter barcodes. Input cells were categorized into four groups: matched with starter cells
296 expressing unique barcodes, matched with starter cells expressing non-unique barcodes, unmatched
297 (unable to find corresponding starter cells), and those with multiple barcodes.

298 In Extended Data Fig. 4e, unmatched input cells were further subdivided based on decoding
299 completeness. Cells that could not be fully decoded due to missing cycles were labeled as “not fully
300 decoded”. The information for all connection-detected cells is provided in the supplementary file,

301 T_connection_3mice.xlsx.

302

303 **Connectivity data processing**

304 **Spatial distribution analysis**

305 The anterior-posterior (AP) distance for each input-starter cell pair was calculated by directly
306 subtracting the x-axis coordinate values of the two cells.

307 For lateral-medial (LM) distance calculations, a perpendicular line was drawn from each starter cell
308 to the pial surface. The LM distance was defined as the shortest distance from the input cell to this
309 perpendicular line. Additionally, the length of this line, extending from the starter cell to the pial
310 surface, was recorded as the depth.

311 The territory of each starter cell was determined as the smallest ellipsoid encompassing 90% of the
312 input cells, with the centroid of the ellipsoid aligned with the location of the starter cell.

313 **Regional connectivity analysis**

314 All connected starter and input cells were automatically annotated to the Allen Brain Atlas based on
315 their spatial coordinates. To ensure consistency, several subregions were manually merged (e.g.,
316 LGd-co, LGd-ip, and LGd-sh were combined into dLGN). The connections between these regional
317 pairs were quantified (Extended Data Fig. 6 and 7a).

318 Randomized shuffle data were generated by randomly pairing existing starter cells with input cells,
319 with 1,000 iterations of shuffling performed. For each regional pair, the statistical difference was
320 calculated by comparing the observed connection value to the distribution of the 1,000 shuffled
321 values using a Z-test. To account for multiple comparisons across all input-starter pairs, p-values
322 were adjusted using the False Discovery Rate (FDR) correction with the Benjamini-Hochberg
323 method.

324 **Co-innervation analysis**

325 When two input cells projected to the same region, they were considered a co-innervation pair.
326 These pairs were counted and categorized according to the region of the input cells (Extended Data
327 Fig. 8a).

328 To assess the statistical significance of these co-innervation pairs, randomized shuffle data were
329 generated under the same conditions: existing starter cells were randomly paired with input cells.
330 For each input-input pair, the statistical difference was calculated by comparing the observed co-

331 innervation counts to the distribution of the 1,000 shuffled counts using a Z-test. P-values were
332 adjusted using FDR correction with the Benjamini-Hochberg method.

333

334 **Automated FISH system**

335 The system was designed and set up in our laboratory. Key components include a metal sand bath
336 (DLAB, HB120S), 24V peristaltic pumps and controller (Runze Fluid, MC20A), electric linear
337 actuators (24V, 4mm/s, 50N, with a 50mm work distance), and syringes for the micro-fluid injection
338 system. The system is controlled by a microcontroller (Arduino, Mega2560) and a real-time clock
339 module (DS3231) for precise timing. A four-digit digital tube display (TM1637) provides additional
340 information for debugging. The custom-designed PCB board (design files provided in
341 supplementary materials, manufactured by Jeipei) controls the system, and an electromagnetic valve
342 (Wokun Technology, WK07-308-3/4-NO) regulates fluid flow. The syringe brackets were 3D
343 printed using #8200 plastic (Wenext). The controller is housed in a custom-designed stainless-steel
344 enclosure (SUS304). All components are mounted on a 33U removable cabinet for easy access and
345 maintenance.

346

347 1 Wang, Q. et al. The Allen Mouse Brain Common Coordinate Framework: A 3D Reference Atlas.
348 Cell **181**, 936-953 e920, doi:10.1016/j.cell.2020.04.007 (2020).

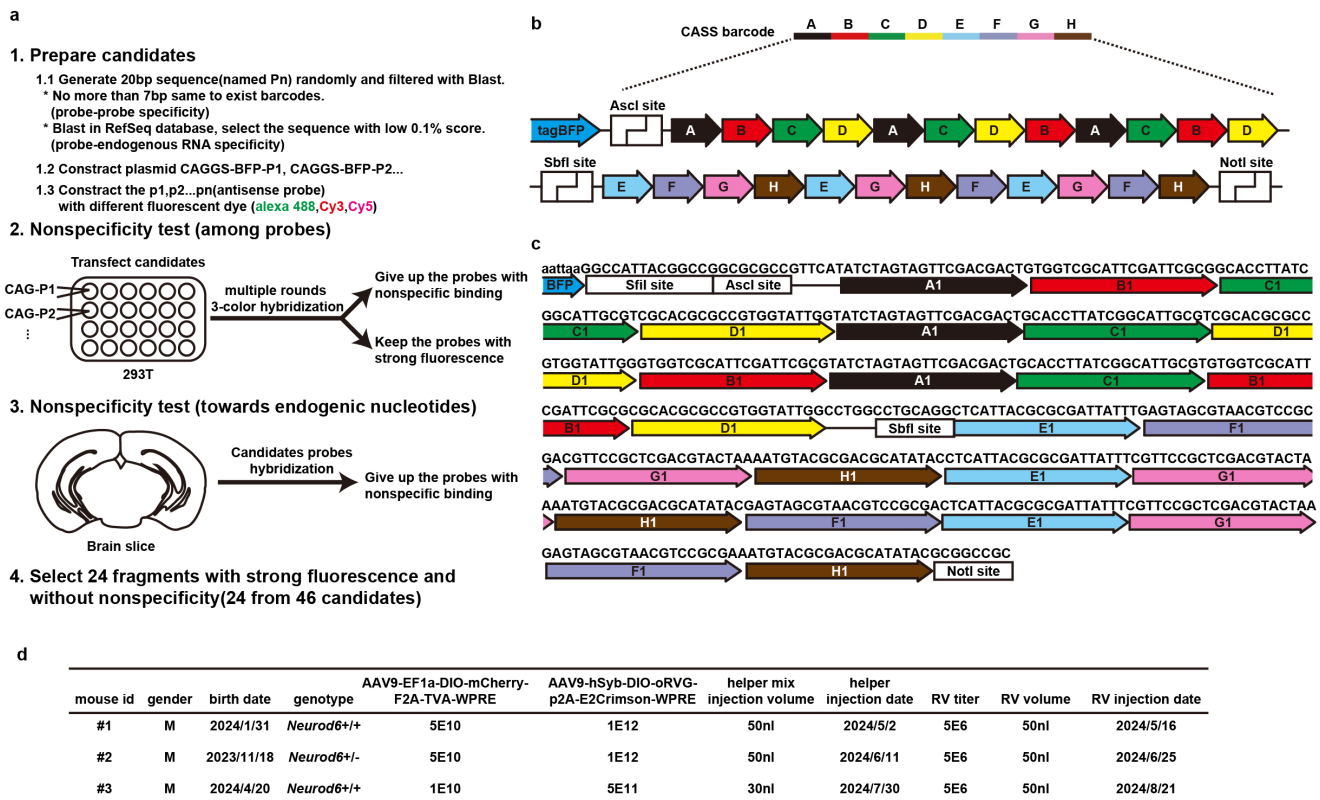
349 2 Puchades, M. A., Csucs, G., Ledergerber, D., Leergaard, T. B. & Bjaalie, J. G. Spatial
350 registration of serial microscopic brain images to three-dimensional reference atlases with the
351 QuickNII tool. PLoS One **14**, e0216796, doi:10.1371/journal.pone.0216796 (2019).

352 3 Stringer, C. & Pachitariu, M. Cellpose3: one-click image restoration for improved cellular
353 segmentation. 2024.2002.2010.579780, doi:10.1101/2024.02.10.579780 %J bioRxiv (2024).

354 4 Hao, Y. BrainMesh: A Matlab GUI for rendering 3D mouse brain structures, <
355 <https://github.com/Yaoyao-Hao/BrainMesh/>> (2020).

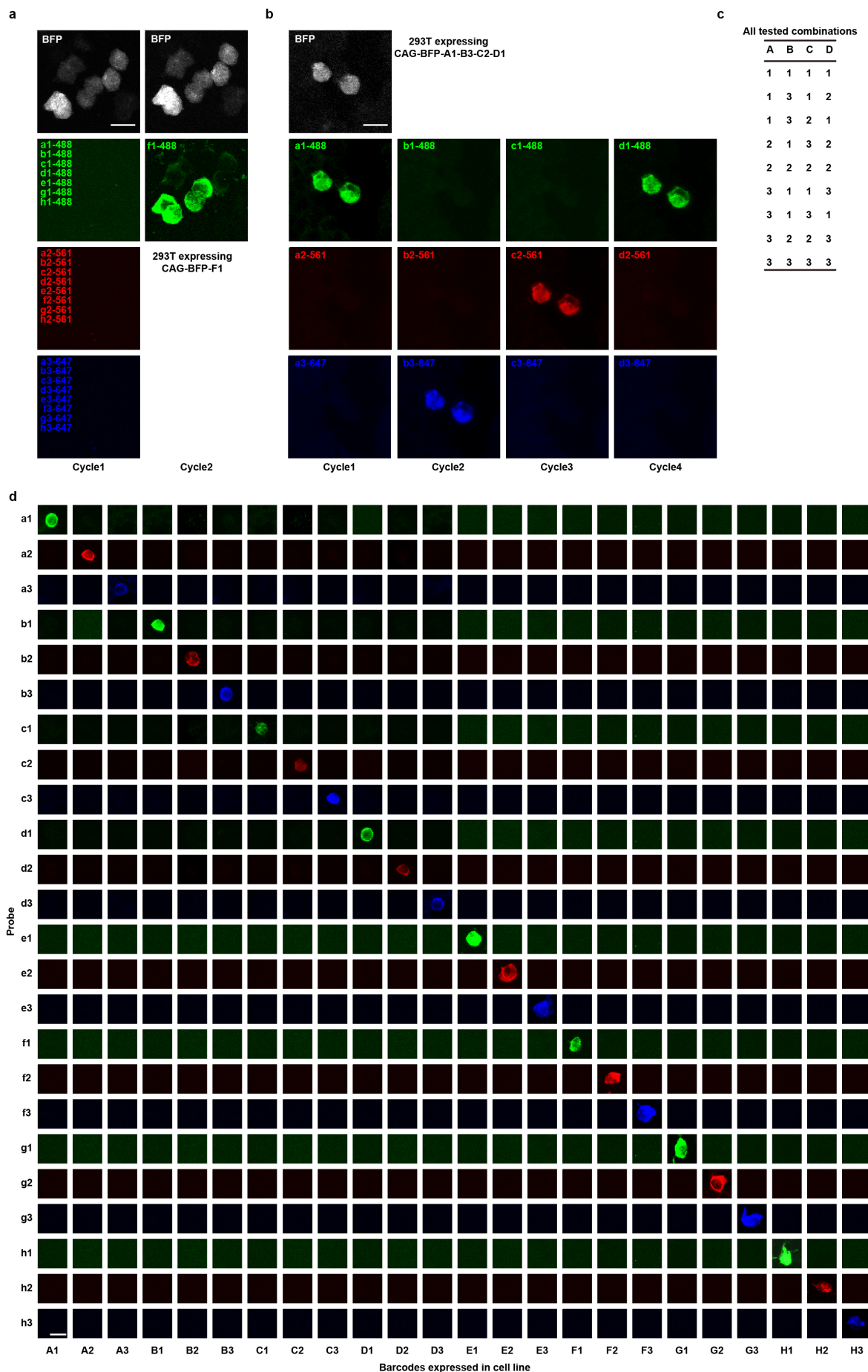
356

357 **Supplementary figures:**



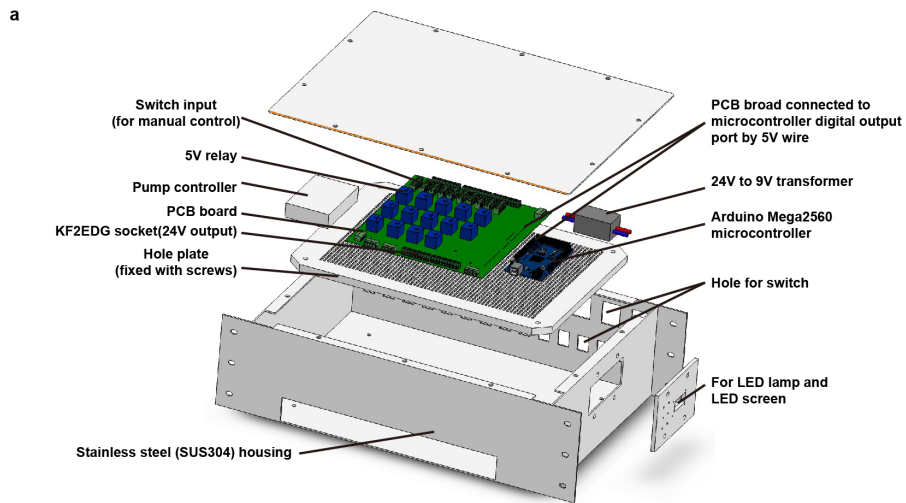
Extended Data Fig. 1 Details of CASS Barcode Design and Experimental Setup

- Process for generating 24 short artificial nucleotide sequences.
- Full structure of a single barcode located in the 3' UTR region of BFP. Each short sequence appears in triplicate, arranged to minimize potential secondary structures. The middle SbfI site facilitates plasmid pool construction.
- Sequence and annotation of a representative barcode (A1B1C1D1E1F1G1H1).
- Details of mouse experiments and virus injection information.



Extended Data Fig. 2 In Vitro Specificity Testing of Barcodes

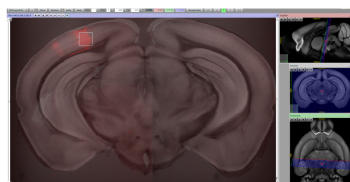
- a. Example of a 2-cycle hybridization test. CAG-BFP-F1 was expressed in 293T cells; the first cycle excluded probe f1, while the second cycle included it. Scale=20 μ m.
- b. Specificity testing with a partial CASS barcode (AnBnCnDn). The barcode was expressed in 293T cells and analyzed via a 4-cycle FISH decoding process, demonstrating high specificity. Scale=20 μ m.
- c. Comprehensive testing with nine variants of partial CASS barcodes to assess probe specificity. Related to b.
- d. Summary of specificity testing, including results from 2-cycle hybridization (a) and 4-cycle FISH decoding (b, c), confirming high specificity for all probes to their corresponding sequences.



b

1. Raw data from confocal microscope

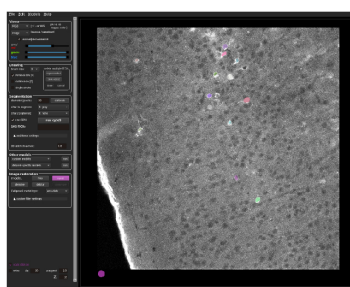
2. Register to Allen brain atlas(mouse V3 2017) by QuicKNI(NITRC tools)



→ Get the transform matrix (for each slice)

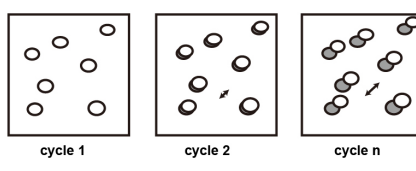
$$[xq \ yq \ zq] = [x/w \ y/h \ 1] \times \begin{bmatrix} ux & uy & uz \\ vx & vy & vz \\ ox & oy & oz \end{bmatrix}$$

3. Cellpose3 Z-stack segmentation (for each view) using pre-trained custom model



→ Get the mask

4. 8-cycle images registering by Matlab



Multicycle XYZ shift correction

5. Semi-automatic barcode decoding by matlab

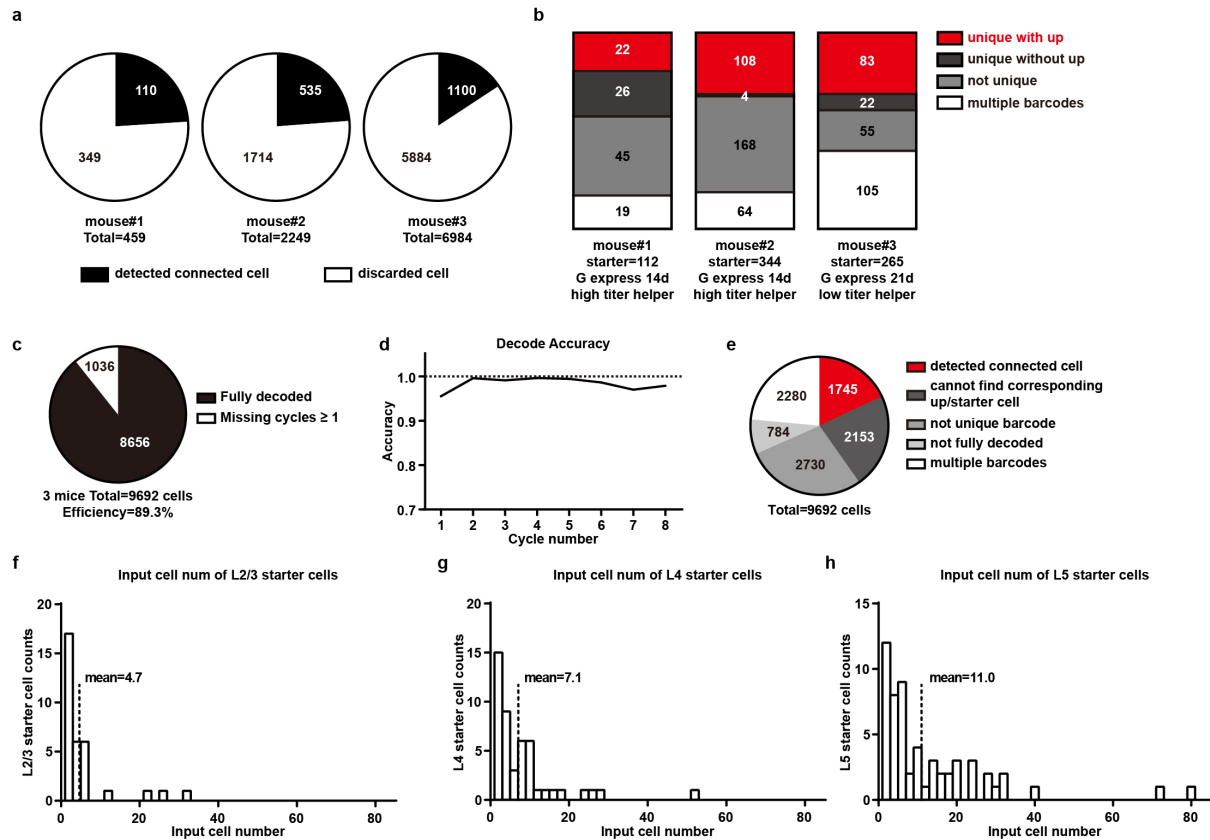
- Select the background ROI
- Calculate the score of all channels in each cell = mean intensity/background Std and get the xyz position of each cell
- Compare the score of each channel and get the decoding result(1,2,3,0,or multiple) and reliability
 - * high reliability(example a1)>2 and [Score_{a1}>2] and [Score_{a2}>2*(Score_{a1}+Score_{a3})] and [Score_{a2}<1] and [Score_{a3}<1]
- Manual check the decoding result

6. Transform the xyz position to Allen brain atlas

$$[xa \ ya \ za \ 1] = [xq \ yq \ zq \ 1] \times \begin{bmatrix} 0 & 0 & 25 & 0 \\ -25 & 0 & 0 & 0 \\ 0 & -25 & 0 & 0 \\ 13175 & 7975 & 0 & 1 \end{bmatrix}$$

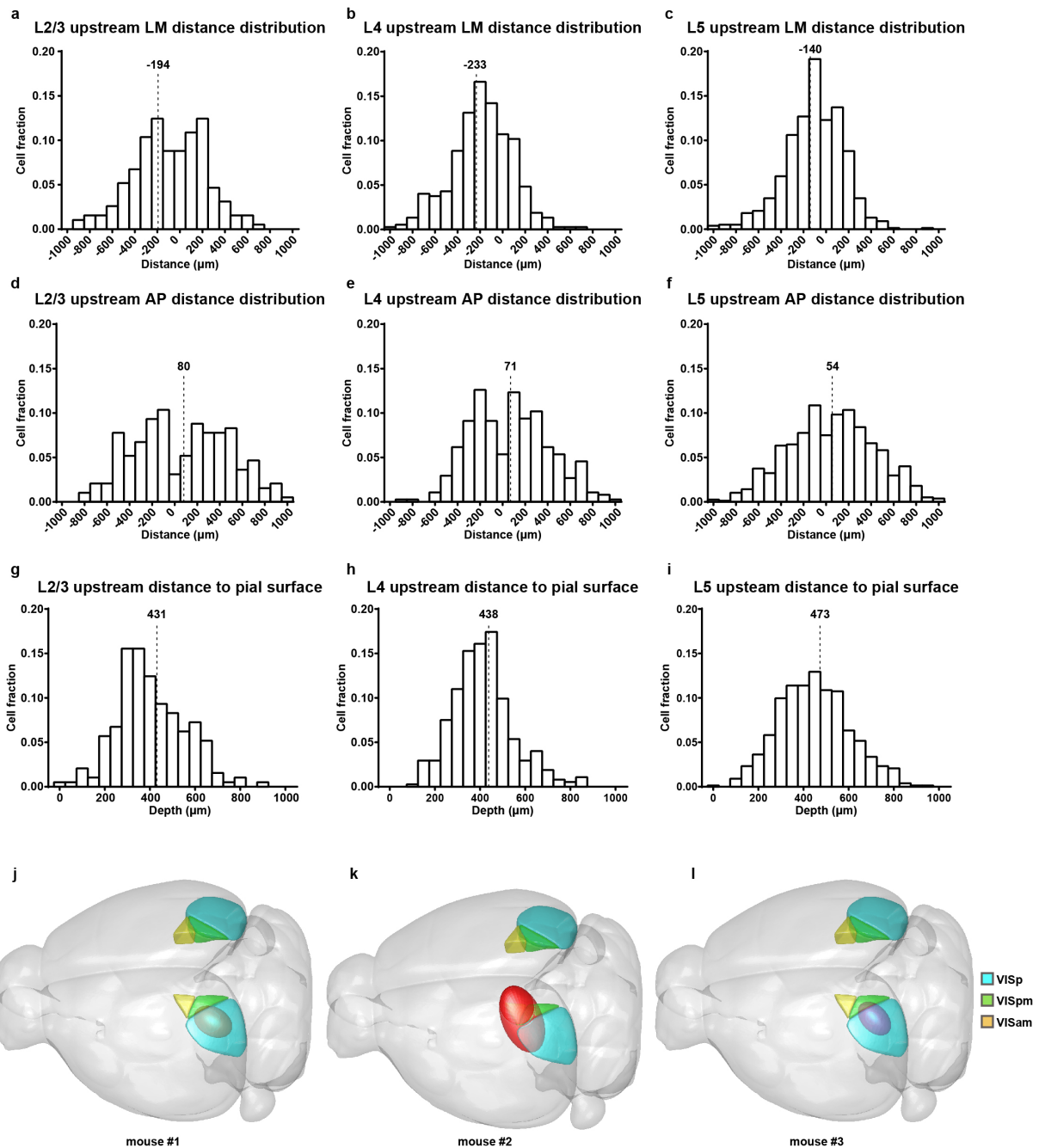
Extended Data Fig. 3 Semi-Automated FISH System and Data Processing

- a. Schematic of the microcontroller-based control system used in the semi-automated FISH system. Wires and switches are not shown.
- b. Details of cell detection and atlas alignment. The XYZ shift in our setup was around 10 μm , basic imaging registration algorithm in Matlab was used and yielded reliable results.



Extended Data Fig. 4 Overview of Detected Cells

- Proportion of connected and discarded cells for each mouse sample.
- Distribution of starter cell categories across mouse samples.
- Decoding efficiency for all detected cells.
- Decoding accuracy for all detected cells in each cycle. Accuracy is defined as the fraction of cells that are fully decoded in each cycle.
- Classification of all detected cells into various conditions. Only cells in the black group (“detected cells”) were included for connection detection. Fault-tolerant algorithms allowed some partially decoded cells to be identified as connected cells or carrying not unique barcodes (see method). The “cannot find corresponding input/starter cells” group here only includes fully decoded cells.
- h. Distribution of input cell numbers across starter cells, grouped by cortical layers.



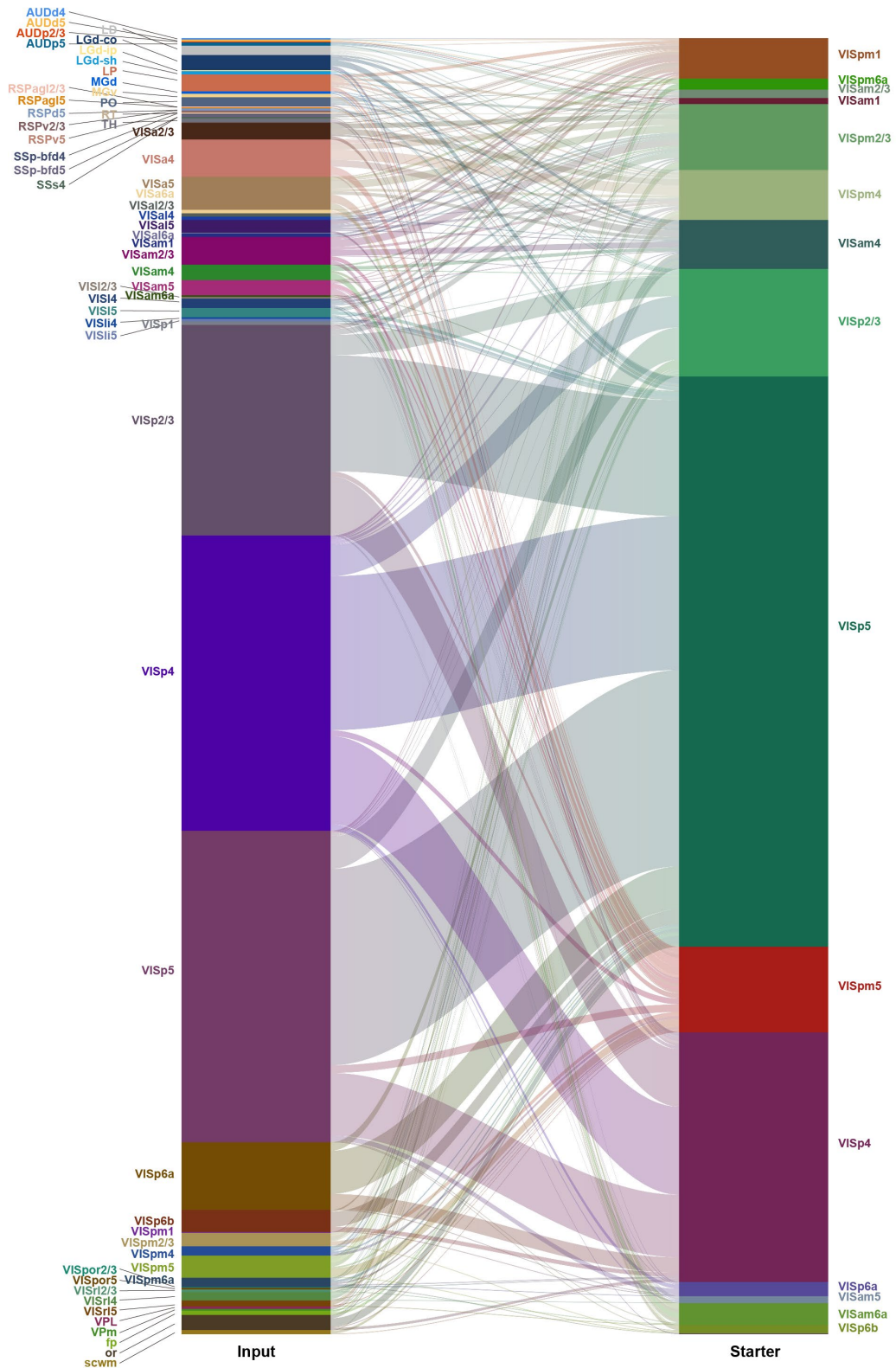
Extended Data Fig. 5 Spatial Organization of Input Cells

a-c. Input cell distribution along the lateral-medial axis, grouped by starter cell layers.

d-f. Input cell distribution along the anterior-posterior axis, grouped by starter cell layers.

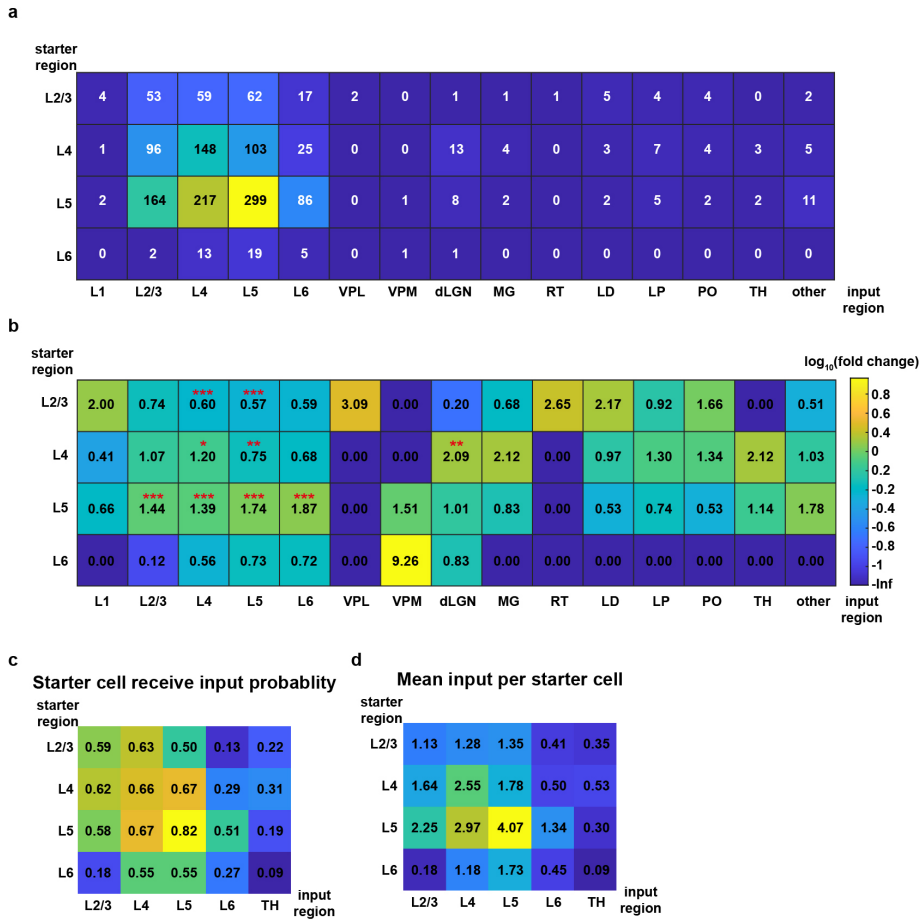
g-h. Distribution of input cell depths relative to the pial surface, grouped by starter cell layers.

i-l. Mean input territories of starter cells for individual experiments, including mouse #2 (injection site covering V1 and V2) and mice #1 and #3 (injection sites in central V1).



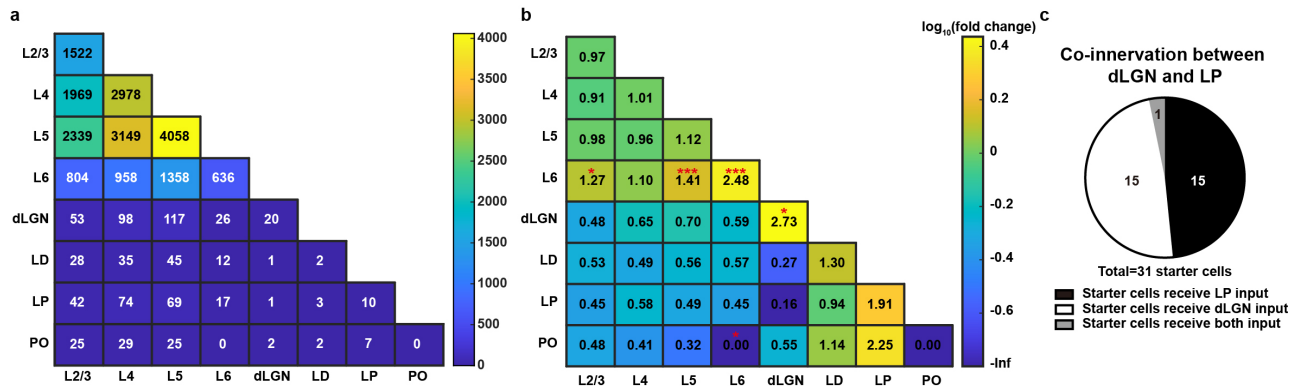
Extended Data Fig. 6 Sankey Diagram of Detected Connections

Connections between upstream and starter cells are represented as lines, with line thickness corresponding to connection strength (i.e., the number of connections). Brain regions are annotated according to the Allen Brain Atlas and are color-coded.



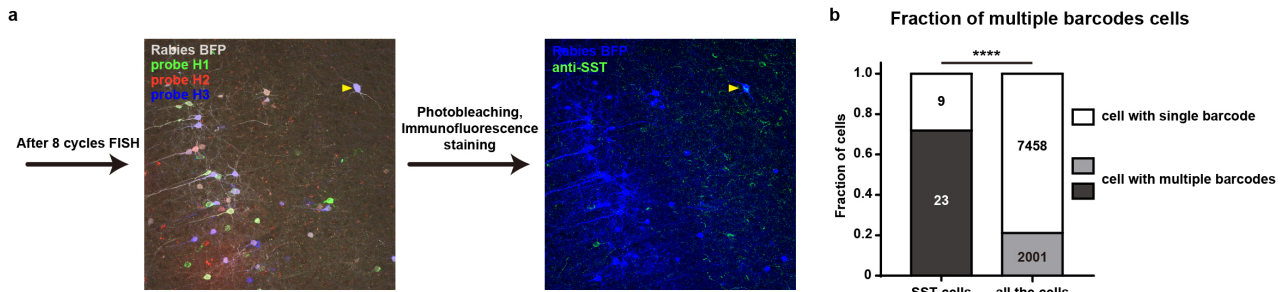
Extended Data Fig. 7 Connectivity Matrix

- Observed counts of connections between brain regions.
- Extended connectivity matrix, showing fold changes (observed/shuffled) as numbers and log10 fold changes as colors. Statistical analysis used Z-tests and FDR correction (Benjamini-Hochberg); *p < 0.05, **p < 0.01, ***p < 0.001. Shuffle iterations = 1000.
- Probability of starter cells receiving input from various brain regions, with TH representing thalamic subregions.
- Average number of input cells per starter across brain regions.



Extended Data Fig. 8 Co-Innervation Preferences of Input Cell Pairs

- Counts of observed co-innervated pairs.
- Observed co-innervation pairs compared with randomized data. Fold changes are shown numerically, and \log_{10} fold changes are indicated by color. Statistical analysis used Z-tests and FDR correction; * $p < 0.05$, ** $p < 0.01$, *** $p < 0.001$. Shuffle iterations = 1000.
- Proportion of starter cells receiving input from dLGN and LP regions.



Extended Data Fig. 9 SST Neuron Identification by Immunofluorescence after barcode decodings

- Immunofluorescence labeling performed after 8-cycle FISH.
- Proportions of cells expressing multiple barcodes among SST neurons and all detected cells.